https://doi.org/10.55972/spectrum.v27i1.451

ORIGINAL PAPER

Spectrum - The Journal of Operational Applications in Defense Areas

Journal homepage: https://spectrum.ita.br

Weapons Systems and Space Applications: Systems Engineering

Prediction of High-Explosive Detonation Effects on Steel Sheets During Experimental Tests Using Finite Element Analysis

Anselmo S. Augusto[1*], Fausto B. Mendonça[1], Girum Urgessa[2], Jose A. Fritz Fidel Rocco[1] and Koshun Iha[1]

[1]Instituto Tecnológico de Aeronáutica, São José dos Campos/SP – Brazil
[2]Howard University, Washington/DC - USA

[*]Corresponding Author: anselmoaugusto@hotmail.com

Keywords

Blast Effects
Structural Response to Explosions
Finite Element Method (FEM)
Dynamic Analysis

Article Information

Received 16 July 2026
Revised 03 August 2026
Accepted 07 August 2026
Available 10 August 2026

Abstract

Investigating the effects of high explosives on metallic structures is important for the development of new protective systems and for assessing the load-bearing capacity of existing structures. To achieve these objectives, a series of detonation tests using TNT charges will be conducted to evaluate the resulting effects on 2 mm-thick A36 structural steel sheets. However, before performing the experimental tests, it is essential to accurately predict the effects of the detonations on the steel sheets in order to ensure test safety and verify that the selected explosive configurations produce the intended structural response. To accomplish this, a series of finite element method (FEM) simulations was carried out using Abaqus®, considering different expected standoff distances. The numerical results indicated that the steel sheets experienced permanent deformations exceeding the material's elastic limit without reaching failure. These findings satisfy the objectives of the study, since either negligible or catastrophic deformations would prevent the proper measurement and evaluation of blast effects on the structural elements during the experimental campaign.

1. Introduction

This document illustrates the standard layout for a Spectrum article. Submitted articles must adhere to a page count ranging from a minimum of five to a maximum of eleven pages.

1.1. Contextualization

The use of explosives is widespread across several fields of human activity, including civil, military, and aerospace applications [1], [2]. Furthermore, there is growing global concern regarding the effects of terrorist attacks [3], [4]. Beyond their intended applications, explosives possess significant destructive potential when used improperly, whether in accidental explosions, terrorist incidents, or improperly executed military operations. Consequently, researchers, have devoted considerable effort to numerous civilian and military institutions, as well as investigating the destructive effects of explosives on both the human body and engineering structures [5], [6].

Among the elements that may be affected by explosive events, civil, military, and aerospace structures are of particular importance. These facilities are continuously exposed to military operations, terrorist attacks, and accidental explosions. The potential destruction of such structures results not only in substantial economic losses but also in material damage and loss of human life [6], [7]. Therefore, investigating the effects of explosives on engineering structures is important for two main reasons: the design of blast-resistant facilities and the appropriate selection of munitions for military operations targeting strategically valuable assets [5], [7].

This study is a continuation of the research conducted by Mendonça et al. [7] – [14] and Augusto et al. [15], [16].

The peer review process was coordinated, and the final publication approved, by Humberto Baldessarini Pires.

1.2. Objectives

In the study presented by Augusto et al. [16], finite element method (FEM) simulations were performed to determine the most appropriate steel sheet thickness and standoff distance for the experimental tests. Based on those results, A36 structural steel sheets with an average thickness of 2.14 mm were selected, and standoff distances ranging from 300 mm to 600 mm were established. Under these conditions, the experimental tests are expected to produce results suitable for achieving the objectives of the research.

The present study extends that work by presenting the results of FEM simulations that more closely represent the actual field test conditions. The main improvements incorporated into the numerical model include modifications to the test support, removal of the displacement measurement device from the center of the steel sheet, definition of the sheet thickness as 2 mm, adjustment of the clear span to 431 mm, and the adoption of a 327 g TNT charge. By reproducing the experimental configuration more accurately, these simulations provide better support for the detonation team during field testing, enabling them to verify whether the tests are being conducted as planned. They also make it possible to assess whether the explosive charge was properly initiated, whether the selected standoff distances are appropriate, and whether the explosive charges are performing within the expected parameters.

Four FEM simulations were performed by varying the distance between the steel sheet and the center of the detonation from 300 mm to 600 mm in increments of 100 mm. The primary output parameter evaluated was the displacement at the center of the steel sheet.

The analyses were performed using the Abaqus® Explicit module, which is suitable for highly dynamic simulations. The simulation workflow was automated through a Python macro developed specifically for Abaqus®. This macro enabled automatic modification of the model configuration, execution of the FEM simulations, extraction of the relevant results, and generation of displacement-versus-distance graphs [17], [18].

2. Materials and Methods

2.1. Constitutive Material Model

The Johnson–Cook (JC) constitutive model [19] was adopted in the present study to characterize the behavior of the steel sheet. This constitutive model, developed in 1983, describes the mechanical response of metals subjected to different temperatures, large strains, and high strain rates. It is particularly suitable for situations in which a ductile material undergoes large deformations under high loading rates, such as those generated by explosive events. Eq. (1) presents the Johnson–Cook formulation for the Von Mises equivalent stress, which accounts for both the strain-rate effect and the reduction in the metal strength due to temperature [19]. In the present study, however, the effect of temperature was neglected in the simulations, in accordance with the findings reported in [20] and [21].

$$\sigma_v = (A + B\varepsilon^n)(1 + C \ln \dot{\varepsilon}^*)(1 - (T_m^*)^m) \quad (1)$$

where:

σ_v – Von Mises equivalent stress;

ε – Equivalent plastic strain;

$\dot{\varepsilon}$ – Strain rate;

$\dot{\varepsilon}^*$ – Dimensionless equivalent strain rate, defined as $\dot{\varepsilon}/\dot{\varepsilon}_0$;

$\dot{\varepsilon}_O$ – Reference strain rate (s^{-1});

A, B, C, n e m – Material constants determined experimentally for each material; and

T_m^* – Homologous temperature.

Following the same theoretical framework, Johnson and Cook later proposed an additional constitutive model [22] incorporating failure in metals. This model accounts for the progressive accumulation of damage throughout the integration cycles of the numerical simulation. The equivalent plastic strain at failure is given by Eq. (2)

$$\varepsilon_{fp} = (D_1 + D_2 e^{D_3 \sigma^*})(1 + D_4 \ln \dot{\varepsilon}^*)(1 + D_5 T^*) \quad (2)$$

where:

ε_{fp} – Equivalent plastic strain at failure;

D_1 to D_5 – Damage constants determined experimentally for each material;

σ^* – Dimensionless stress, defined as σ_m/σ_v; and

σ_m – Mean stress, calculated as the average of the three principal stresses.

Since the value of ε_{fp} given in Eq. (2) varies throughout the analysis, it is necessary to define a damage variable (D) that accumulates damage over the integration cycles of the numerical model, as expressed in Eq. (3). When this variable reaches a value of 1, the material is considered to have failed.

$$D = \sum \frac{\Delta\varepsilon_p}{\varepsilon_{fp}} \quad (3)$$

where $\Delta\varepsilon_p$ is the increment of equivalent plastic strain accumulated during each integration cycle.

2.2. Detonation Tests at the Test Arena

The experimental tests are scheduled to be conducted at the detonation test range of the Instituto de Aeronáutica e Espaço (IAE). The proposed test configuration is shown in Fig. 1. A steel support structure, 900 mm in height, will be anchored to a concrete foundation. This structure was designed to be sufficiently rigid so that no significant deformation occurs during the blast tests. Bare spherical TNT charges with a diameter of 75 mm and an average mass of 327 g will be used. A36 steel sheets measuring 600 × 400 × 2.14 mm will be replaced after each test. These sheets are fabricated with folded edges and bolt holes for attachment to the support structure. They will be secured using thick steel clamping bars and six bolts. The clear span of the steel sheet subjected to the blast loading will be 431 mm. The resulting deformations will be measured using a high-speed camera positioned at a safe distance.

During the experimental campaign, the distance from the

center of the explosive charge to the front surface of the steel sheet will vary from 300 mm to 600 mm.

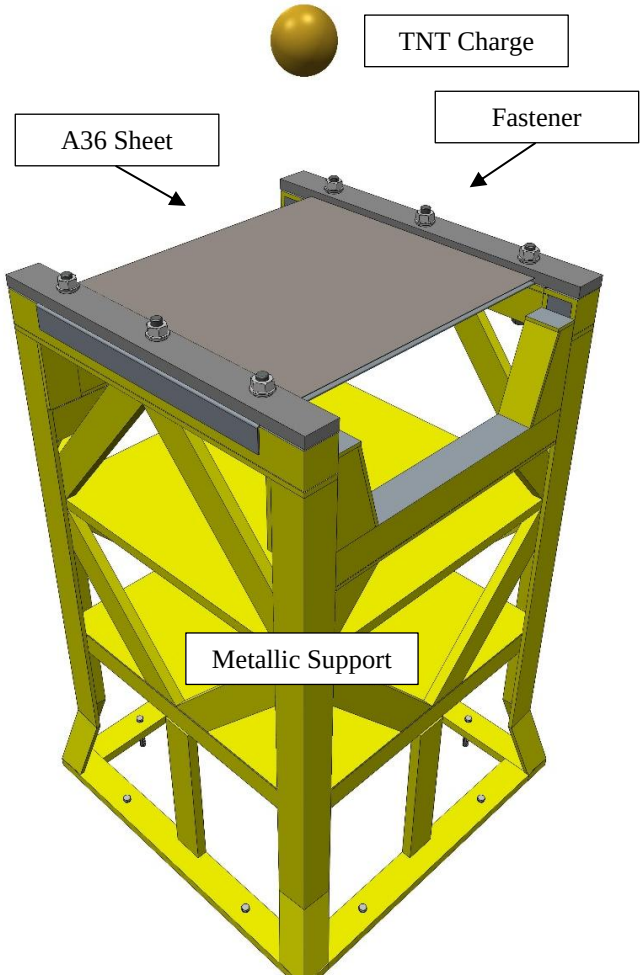


Fig. 1. Tests Layout.

2.3. FEM Modeling of the Detonation Test

To represent the A36 steel sheets, four-node reduced-integration Lagrangian shell elements (S4R) were employed, considering their small thickness relative to the other dimensions. The Johnson–Cook (JC) constitutive model, described previously in Section 2.1, was adopted. The JC material parameters for A36 steel were obtained from the literature [23], [24] and are summarized in Table I.

Table I. Johnson–Cook Parameters for A36 Steel [23], [24].

Dimensional		***Dimensionless***	
Density (kg/m³)	7,850	ν	0.26
E (GPa)	200	n	0.228
A (MPa)	285.9	m	0.917
B (MPa)	499.8	C	0.0171
Tm (K)	1,811	D1	0.4025
To (K)	300	D2	1.107
$\dot{\varepsilon}_0$	1.00	D3	-1.899
		D4	0.00961
		D5	0.3

Appropriate boundary conditions were applied throughout the simulations.

To calculate the blast loads acting on the steel sheet, the CONWEP [25] plug-in available in Abaqus® was used. This tool is widely validated for free-air blast loading and is based on the empirical Kingery–Bulmash equations [26], which are adopted in several defense manuals and by international institutions [6], [27].

The finite element mesh had an average element size of approximately 3 mm, resulting in models with 23,810 nodes and 23,454 four-node linear quadrilateral shell elements (S4R). Mesh refinement studies using a 2 mm element size did not improve the numerical results and only increased the computational cost.

Fig. 2 shows the final simulation model implemented in Abaqus®, while Fig. 3 presents details of the mesh refinement. Since the folded edges of the steel sheet do not influence the experimental results, they were omitted from the numerical model.

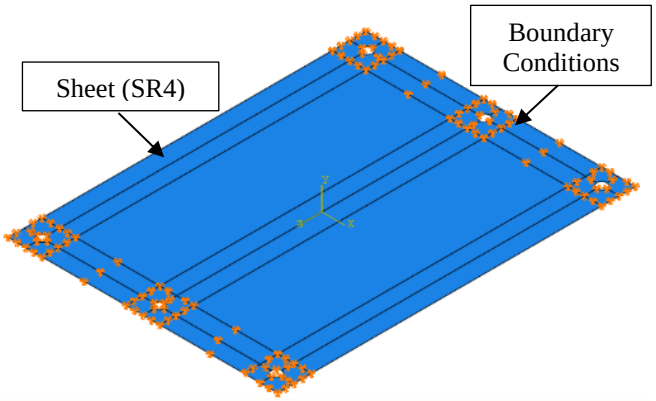


Fig. 2. FEM Simulation Model Implemented in Abaqus®.

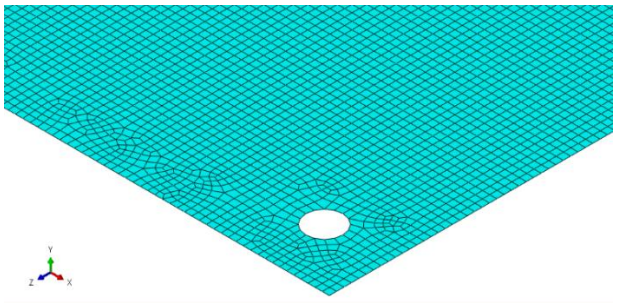


Fig. 3. Mesh Refinement Details.

2.4. Simulation Procedure

Each simulation covered a period of 100 ms after detonation, which was sufficient to capture the primary response of the steel sheet. The average processing time was approximately 2.5 hours per simulation using four parallel 2.2 GHz processors and 16 GB of RAM.

Four simulations were performed for standoff distances ranging from 300 mm to 600 mm, with increments of 100 mm.

A Python macro was specifically developed for Abaqus® to automatically modify the model parameters for each case, execute the simulations, open the output database files, extract the relevant results, and export the numerical data and image files. The total computational effort required to complete all simulations was approximately 10 hours.

3. Results and Analysis

3.1. Results

A summary of the main results obtained from the simulations is presented in Table II. The meaning of each parameter is described in the following paragraphs.

One of the most relevant output parameters is the displacement (*U*) at the center of the steel sheet. This displacement is commonly used to predict the level of structural damage, as established by [5] and [6]. Fig. 4 illustrates the displacement histories at the center of the steel sheet for each standoff distance. Downward displacement, corresponding to the direction of blast-wave propagation, is considered negative. *Umin* denotes the maximum downward displacement experienced by the center of the sheet immediately after the arrival of the blast wave. In contrast, *Umax* represents the maximum positive displacement that occurs as the sheet vibrates and temporarily moves upward. Due to material damping and permanent plastic deformation, the magnitude of *Umin* is always greater than that of *Umax*.

The time required for the sheet to reach *Umin* is denoted by *t Umin*. Fig. 5 presents isometric views of the deformed steel sheets for each standoff distance, showing the displacement (*U*) at a simulation time close to *t Umin*.

Another parameter of major importance is the Equivalent Plastic Strain (PEEQ), which represents the permanent deformation accumulated beyond the elastic limit of the material. Higher PEEQ values indicate more severe irreversible damage. Fig. 6 shows the maximum accumulated PEEQ over the entire simulation for each standoff distance, presented in a top view of the steel sheet.

PEEQmaxt and *PEEQmaxc* denote the maximum equivalent plastic strain observed over the entire steel sheet and at its center, respectively.

The last mechanical parameter evaluated, although not discussed in detail in this study, is the equivalent stress, or Von Mises stress, experienced by the steel sheet *MISESmaxt* and *MISESmaxc* represent the maximum Von Mises stress over the entire sheet and at its center, respectively.

Table II. Results Summary

		Standoff distance of the detonation (mm)			
Parameter	**Unit**	**300**	**400**	**500**	**600**
U min	**(mm)**	-47.24	-36.01	-28.74	-23.83
t Umin	**(ms)**	0.96	1.06	1.16	1.28
U max	**(mm)**	-	-	-	13.07
|V max|	**(m/s)**	73.99	48.85	39.38	33.92
|A max|	**(m/s^2)**	1.61E+06	1.18E+06	5.33E+05	3.43E+05
PEEQmaxt	**%**	23.04	18.93	17.43	11.81
PEEQmaxc	**%**	5.19	3.79	4.32	4.33
MISESmaxt	**MPa**	683.20	663.92	652.55	623.44
MISESmaxc	**MPa**	571.54	553.88	560.18	553.56

Finally, |V max| and |A max| denote the maximum magnitudes of the velocity and acceleration, respectively, recorded at the center of the steel sheet.

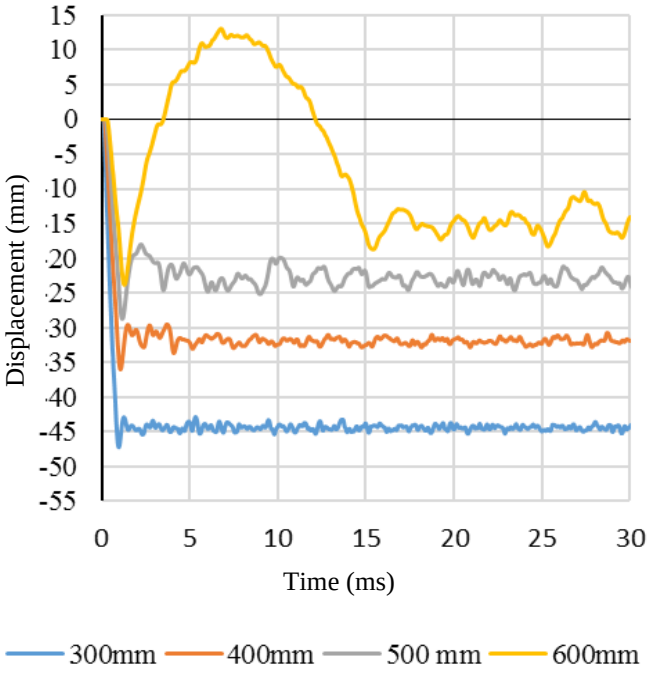


Fig. 4. Displacement at the center of the steel sheet as a function of time for different standoff distances.

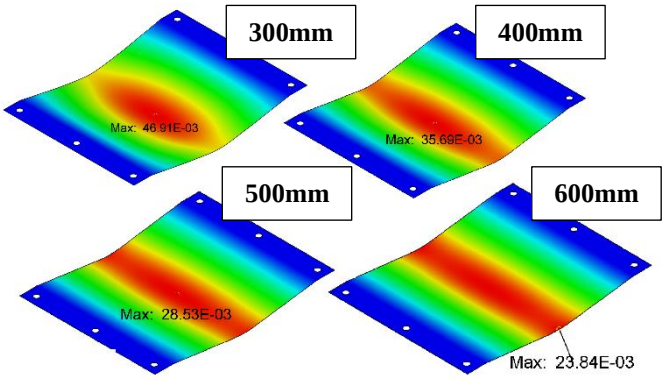


Fig. 5. Deformed shapes of the steel sheets at the instant of maximum recorded displacement in the simulation for each standoff distance (highlighted in the insets). Isometric view.

3.2. Analysis

The primary objective of this study is to predict the effects of TNT charges on steel sheets before conducting full-scale blast experiments. The main simulation results are summarized in Table II. As expected, the closer the detonation is to the steel sheet, the more severe the resulting structural response.

The displacement histories shown in Fig. 4 illustrate the response at the center of the steel sheet. For standoff distances up to 500 mm, the sheet deformed downward without exhibiting significant oscillatory motion. After reaching a peak downward displacement ranging from 28 to 47 mm, the sheet remained

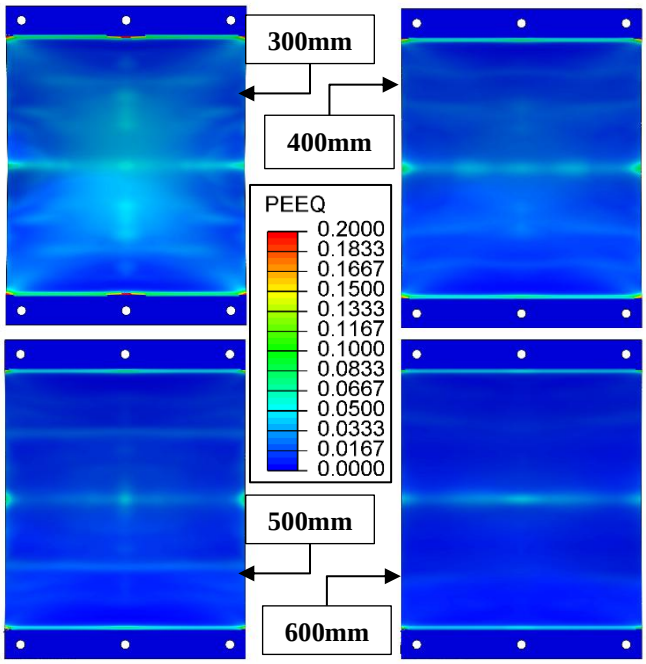


Fig. 6. Accumulated equivalent plastic strain (PEEQ) in the steel sheet throughout the simulation for each standoff distance (highlighted by the arrows in the insets). Top view.

with a slightly smaller permanent downward deformation. In contrast, at the 600 mm standoff distance, the lower blast intensity allowed the sheet to exhibit oscillatory behavior. After reaching a maximum downward displacement of approximately 23 mm, the sheet rebounded upward, reaching a positive displacement of up to 13 mm, before returning downward and stabilizing with a permanent deformation of approximately 15 mm.

This behavior is attributed to the higher levels of plastic deformation produced by the more intense blast loads. Under these conditions, the material loses much of its ability to recover its original shape. At the largest standoff distance, however, the elastic response of the steel sheet remained significant, resulting in the oscillatory behavior expected under lower deformation levels.

The equivalent plastic strain (PEEQ) results indicate that permanent deformation occurred over several regions of the steel sheet, becoming more pronounced as the detonation distance decreased. As shown in Fig. 6, the highest PEEQ values were concentrated near the sheet supports. Therefore, although the largest displacements occurred at the center of the sheet, the rigid boundary conditions produced greater concentrations of plastic strain near the supports, indicating a higher likelihood of failure in these regions.

Further analysis of Table II and Fig. 6 provides an indication of how close the material approached failure. As a reference, A36 steel specimens typically fail at an equivalent plastic strain of approximately 20% [28]. Regions where the accumulated PEEQ exceeded this value are highlighted in red in Fig. 6. Only the simulation with a 300 mm standoff distance produced localized values of PEEQmax above this threshold, indicating a potential risk of rupture, particularly near the supports.

The stress results show that the steel sheet experienced high stress levels, with some regions exceeding the 250 MPa yield strength of A36 steel [28]. Consequently, yielding is expected to occur in all simulated cases, which is consistent with the plastic deformations observed.

Finally, the magnitudes of the velocity, acceleration, and time required to reach the peak displacement at the center of the steel sheet highlight the highly dynamic nature of the blast response. Peak velocities ranged from 33 to 74 m/s, while peak accelerations reached the order of 10^6 m/s². The time required to reach the maximum displacement was on the order of 1 ms, demonstrating the extremely rapid and severe effects produced by the detonation.

4. Conclusions

Based on the results and analyses presented, III, it can be concluded that the selected standoff distances will produce the structural response expected for the experimental campaign. The steel sheets are predicted to undergo significant deformation and damage without being completely ruptured or destroyed.

The primary objective of this study was to predict the structural response during the planned detonation tests, thereby providing support to the field team in identifying any deviations from the expected test conditions during the experimental campaign. It is important to emphasize that explosive testing is costly in terms of materials, personnel, and the infrastructure required to ensure safe operations. In this context, the finite element method (FEM) proved to be an efficient and cost-effective tool, whose predictive capability has already been demonstrated in previous studies, such as [29] and [30].

Conflicts of interest

The authors declare that they have no known competing financial interests or personal relationships that could have appeared to influence the work reported in this paper.

Author contributions

A. S. Augusto: Conceptualization, Methodology, Validation, Formal analysis, Investigation, Resources, Data curation, Writing – original draft, Visualization, Project administration; **F. B. Mendonça:** Conceptualization, Methodology, Writing – review and editing, Visualization; **G. Urgessa:** Conceptualization, Methodology, Validation, Resources, Data curation, Writing – review and editing, Visualization, Project administration; **J. A. F. F. Rocco:** Conceptualization, Methodology, Writing – original draft, Visualization; **K. Iha:** Conceptualization, Writing – review and editing, Visualization, Supervision. All authors have read and agreed to the published version of the manuscript.

Data availability

The data that support the findings of this study are not publicly available due to security restrictions, but are available

from the corresponding author upon reasonable request.

Funding information

This research received no external funding.

Acknowledgment

The authors sincerely thank the Instituto de Aeronáutica e Espaço (IAE) for supporting this research by providing the finite element analysis software and for making its detonation test arena available, where the experimental blast tests will be conducted.

References

[1] P. W. Cooper, “Explosives Engineering”, New York: Wiley-VCH, 1997.

[2] Department of the army, “TM 9-1300-214 - Military Explosives, Washington”, D.C.: Department of the army, 1984.

[3] A. Nazarian, C. Presser, "Forensic analysis methodology for thermochemical characterization of ANNM and ANFO homemade explosives," *Thermochim. Acta*, vol. 608, pp. 65-75, 2015.

[4] A. M. Remennikov, “The state of the art of explosive loads characterization”, Wollongong: University of Wollongong, 2016.

[5] D. Cormie, M. Geoff, “Blast effects on buildings”, London: Thomas Telford, 2009.

[6] USDOD, "Structures to resist the effects of accidental explosions - UFC 3-340-02," Department of Defense (USDOD), Washington, 2008.

[7] F. Mendonca, “Avaliação da capacidade do explosivo plástico PBX gerar danos a uma laje de concreto armado biapoiada por efeito de onda de choque”, São José dos Campos: PhD Dissertation in Ciências e Tecnologias Espaciais - ITA, 2017.

[8] F. Mendonca, G. Urgessa, K. Iha, R. Rocha, J. Rocco, "Comparison of Predicted and Experimental Behaviour of RC Slabs Subjected to Blast using SDOF Analysis," *Def. Sci. J.*, vol. 68, no. 2, pp. 138-143, 2018.

[9] F. Mendonça, R. Gonçalves, G. Urgessa, K. Iha, R. Rocha, M. Domingues, J. Rocco, "Emprego de química computacional na verificação e validação da pressão de detonação de explosivo plástico-PBX," *Quim. Nova*, vol. 41, no. 3, pp. 310-14, 2018.

[10] F. Mendonça, G. Urgessa, J. Rocco, "Blast Response of 60 MPa Reinforced Concrete Slabs Subjected to Non-Confined Plastic Explosives," in *Proceedings of the Structures Congress, American Society of Civil Engineer*, Denver, CO, 2017.

[11] F. Mendonça, G. Urgessa, J. Rocco, "Experimental investigation of 50 MPa reinforced concrete slabs subjected to blast loading," *Ingeniería e Investigación*, vol. 38, no. 2, pp. 27-33, 2018.

[12] F. Mendonça, G. Urgessa, R. Dutra, R. Gonçalves, K. Iha, J. Rocco, "EPS foam blast attenuation in full-scale field test of reinforced concrete slabs," *Acta Sci.*, vol. 40, no. 1, p. e40020, 2020.

[13] F. B. Mendonça, G. S. Urgessa, K. Iha, J. A. F. F. Rocco, "Comparação Entre os Critérios de Projeto de Carga de Vento e Efeito Sopro de uma Detonação – Caso das Torres de Alta Tensão," *Spectrum*, vol. 22, no. 1, p. 42–46, 2021.

[14] F. B. Mendonça, K. Iha, G. Pinheiro, C. B. Amorim, J. A. F. F. Rocco, "Comportamento de uma laje de concreto armado submetida aos efeitos da onda de choque oriunda da detonação de explosivo plástico de uso militar," *Spectrum*, vol. 22, no. 1, p. 25–29, 2021.

[15] A. S. Augusto, F. Medonça, G. Urgessa, I. Koshun, "Finite Element Analysis of Experimentally Tested Concrete Slabs Subjected to Airblast," *Defence Science Journal*, vol. 71, no. 5, pp. 630-638, 2021.

[16] A. S. Augusto, F. B. Mendonça, G. Urgessa, K. Iha, "Pre-test input optimization of high explosive blast effects on steel sheets using finite element analysis," in *Proceedings of the Simpósio de Aplicações Operacionais em Áreas de Defesa*, São José dos Campos, 2022.

[17] SIMULIA, "Abaqus Version 6.10," Dassault Systèmes, Vélizy-Villacoublay, 2010.

[18] SIMULIA, "Abaqus Theory Manual Version 6.10," Dassault Systèmes, Vélizy-Villacoublay, 2014.

[19] G. Johnson, W. Cook, "A constitutive model and data for metals subjected to large strains, high strain rates and high temperatures," in *Proceedings of the International Symposium on Ballistics*, 7, The Hague, 1983.

[20] H. Jama, M. Bambach, G. Nurick, et al, "Numerical modeling of square tubular steel beams subjected to transverse blast loads," *Thin-Wall Struct*, vol. 47, p. 1523–34, 2009.

[21] Y. Ding, M. Wanga, Z.-X. Li, H. Hao, "Damage evaluation of the steel tubular column subjected to explosion and post-explosion fire condition," *Engineering Structures*, vol. 55, pp. 44-55, 2013.

[22] G. Johnson, W. Cook, "Fracture characteristics of three metals subjected to various strains, strain rates, temperatures and pressures," *Engineering Fracture Mechanics*, vol. 21, pp. 31-48, 1985.

[23] M. Gomah, M. Demiral, "An Experimental and Numerical Investigation of an Improved Shearing Process with Different Punch Characteristics," *Journal of Mechanical Engineering*, vol. 66, no. 6, p. 2020, 2020.

[24] S.-W. Lee, S.-H. Chang, "Experimental investigation of pull-through force of wing-type fastening inserts co-cured in long fiber prepreg sheet (LFPS)," *Composite Structures*, vol. 206, no. 2018, pp. 978-986, 2018.

[25] D. W. Hyde, "Conventional weapons effect (CONWEP) - Application of TM5-855-1.," Department of the Army, Vicksburg, 1988.

[26] C. N. Kingery, G. Bulmash, "Technical report ARBRL TR-02555 - Airblast parameters from TNT spherical air burst and hemispherical surface burst," Aberdeen Proving Ground, Army Armament and Development Center, Ballistic Research Laboratory, Maryland, US, 1984.

[27] ONU, "Kingery-Bulmash Blast Parameter Calculator," ONU, 2023. [Online]. Available: https://unsaferguard.org/un-saferguard/kingery-bulmash.

[28] ArcelorMittal, "Rolled Products Catalogue - 2015 Edition," ArcelorMittal, Jardim Limoeiro Serra - ES, 2015.

[29] M. Abdallah, "Numerical Study of Steel Structures Responses to External Explosions," in *Proceedings of the International Conference on Civil Engineering and Architecture* 2017, Berlin-Germany, 2020.

[30] E. L. Eskew and S. Jang, "Remaining capacity estimation for buildings after an explosion using the adaptive alternate path analysis," *Advances in Structural Engineering*, vol. 23, no. 4, pp. 630-641, 2019.